Preprints of the 19th World Congress
The International Federation of Automatic Control
Cape Town, South Africa. August 24-29, 2014

A Stitching Method for AFM Based Large Scale Scanning with High Resolution

Sheng Zhao*, Qinmin Yang*

**State Key Laboratory of Industrial Control Technology,
Department of Control Science and Engineering, Zhejiang University,
Hangzhou, Zhejiang 310027 China, (e-mail: qmyang@zju.edu.cn)*

Abstract: Internal nonlinearities within piezoelectric actuators of Atomic Force Microscopes (AFM) still pose a great challenge for practicers in the area of nanotechnology. Especially, when topography of a large scale area is required along with high resolution, traditional scanning protocol will deteriorate the distortion of images. In this paper, a novel block scan and stitching method is proposed to mitigate such phenomena. By dividing the whole area into blocks and integrating them subsequently, creep, hysteresis and thermal drift within images can be reduced largely. Moreover, the whole procedure is executed in an automatic manner without human's intervention. Its feasibility is also verified by real experimental results.

Keywords: Atomic force microscope (AFM), nonlinearities of piezoelectric actuators, phase correlation method.

1. INTRODUCTION

With the invention of scanning probe microscopes (SPMs), to acquire surface topography of objects with nano scale resolution has become possible. Compared with scanning tunnelling microscopy (STM), which has to be run in strict environmental conditions, atomic force microscopy (AFM) provides a convenient channel to deliver nano-scale images in ambient conditions (Binnig, G. et al, 1983).

However, the spatial uncertainties of tip positioning caused by the nonlinear behaviours of the piezoelectric (PZT) ceramic are still a barrier which hinders the accuracy of the image acquired. The most recognized nonlinearities mainly include hysteresis, creep and thermal drift. Essentially, hysteresis leads to inconsistence of displacement curves for same voltage applied. Meanwhile, the displacement needs a long time to keep stable when an abrupt change of voltage is inserted to the PZT because of creep. The effect of temperature jitter will also incur the random thermal drift phenomenon.

At present, to enhance the AFM image quality, numerous efforts are devoted to the compensation of these adverse behaviours (Marinello, F. et al, 2007; Yang, Q. et al, 2008; Mokaberi, B. et al, 2008; Huerth, S.H. et al, 2003). Models of hysteresis and creep have been extensively investigated in literatures (Goldfarb, M, 1997; Mokaberi, B. et al, 2008). Identification of the model parameters are also addressed in these papers. In commercial AFM instruments, hysteresis is reduced by always scanning in the same direction, while creep effects are assumed to almost vanish by waiting a few minutes after a large scanning motion. That is to say, when scanning a large area, the actuator has to pause for a while for the creep to disappear, which results in a decrease of efficiency. Although specific PZT hardware can be utilized for large area scanning with less creep effect, it is more costly and may have problem in achieving high-resolution images.

As to the compensation of drift, Requicha's group has managed to predict and thus reduce the impact by Kalman filter (Mokaberi, B. et al, 2006). Yang turns to neural network for an automatic solution (Yang, Q. et al, 2008). However, all these aforementioned drift compensation methods are concerned to the drift existing between successive images of the same scanning region. The drift happened within each individual image is ignored by assuming that it doesn't take much time to scan a small area. Apparently, for some specific applications which require scanning a large scale region with high resolution, the time consumed to acquire that task is comparatively long, and thus leads to unignorable distortion.

To overcome these problems and obtain a balance between scanning area and resolution, a block scan and stitching method is introduced in this paper. It firstly divides the scan area into small blocks, obtains a high-resolution image of each block in a specific sequence, and then stitches all blocks into a big whole one by using phase correlation method. This methodology can be very helpful when big scale topography with high resolution is needed, and all steps are accomplished in an automatic manner.

The rest of the paper is organized as follows. Section 2 formulates the problem, whereas Section 3 presents the detailed methodology to alleviate it. The implementation and experimental results are given in Section 4 before conclusion.

2. PROBLEM STATEMENT

Although piezoelectric actuators have been widely utilized in Scanning Probe Microscopy (SPM) due to their superior

piezoelectric coefficients, they still exhibit certain nonlinearities including creep, hysteresis, and drift. These phenomena are deteriorated in particular when a large area is scanned, i.e. a large length of movement is required for actuators.

In current AFMs, to obtain the topography of a sample, the scanner moves the probe over the sample surface in a precise, defined pattern known as a raster pattern, a series of rows in a zigzag pattern covering a square or rectangular area. By this means, hysteresis can be mitigated. Besides, the tip has to wait a while for the creep to vanish before each row scan when imaging large areas. Thermal drift between successive images has also been largely investigated and compensated in literatures (Mokaberi, B. et al, 2008; Yang, Q. et al, 2008). However, it is still an open and challenging question on how to eliminate the drift error within an image, which is simply assumed to be neglectable for small imaging areas.

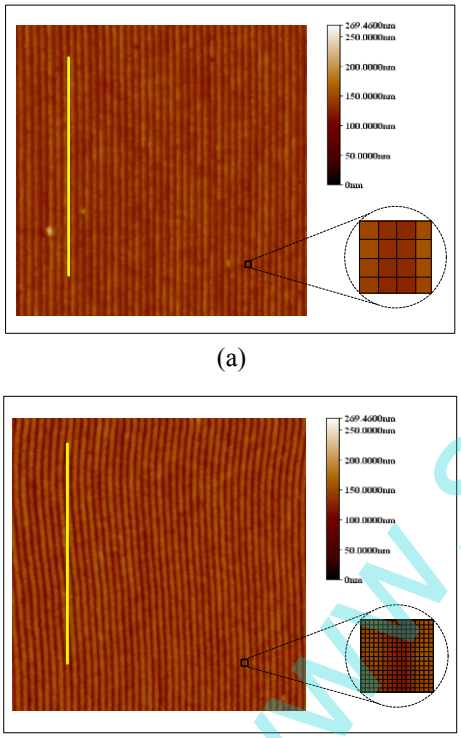

(a)

(b)

Fig. 1. Comparison of a 14um*14um area scanned with different resolution. (a) 1024*1024; (b) 4096*4096.

Therefore, when the topographic information of a large region is demanded along with high resolution, it is evident that traditional scanning method will encounter severe distortion mainly resulted from creep and drift. As illustrated in Fig.1 (a) and (b), the same 14um*14um region of a grating sample is scanned by an AFM with same scan rate of 4Hz but different resolution. In Fig. 1 (a), the topography is obtained with the resolution of 1024*1024, and it takes 256 seconds. Meanwhile, Fig. 2 (b) shows the image with resolution altered to 4096*4096 and it costs 256*16 seconds to finish one imaging routine. It can be readily found that the first topography is more obscure than the second one due to resolution difference. On the other hand, the veins of the first image are almost straight while the second one is apparently distorted as a result of drift, since it takes much more time than the first one. Thus, it becomes a struggling tradeoff between image quality and resolution for AFM users. A method to achieve satisfactory performance on both of them is strongly desired.

3. BLOCK SCAN AND STITCHING METHODOLOGY

In this section, a methodology based on block scan and stitching technique is introduced to acquire topography of large areas along with high resolution while the drift and creep effects are largely compensated.

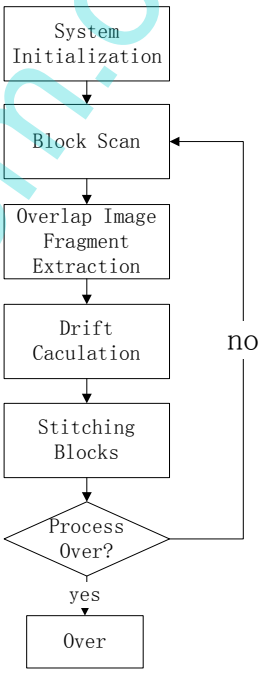

Fig. 2. The flow diagram of the block scan and stitching methodology.

The flow diagram of the proposed scheme is depicted in Fig. 2. The entire scheme will operate in a recursive way until the image of the entire region to be scanned is retrieved. Firstly, the whole area is divided into blocks overlapping with each other. The blocks have relatively small size but high resolution. Thus, it will not incur much creep and drift distortion within each block. Subsequently, imaging of each of them is conducted in a predefined order. The overlapping areas between successive blocks are identified by using phase correlation method. The drift happened between them is also estimated and further compensated. Eventually, all blocks are combined (stitched) together to form a topographic description of the original large region along with high resolution. Therefore, by using the proposed block scan and stitching methodology, a large scale image can be obtained without sacrificing resolution or hurting image quality. Furthermore, all steps are conducted automatically.

3.1 Block Scan

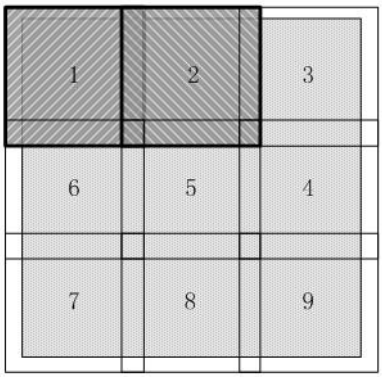

Fig. 3. An example of partitioning large scanned region into 9 blocks. The dark area denotes the region to be imaged.

First of all, the entire image has to be divided into multiple smaller square or rectangular blocks. Two parameters have to be determined in advance, including block size and resolution. The latter is usually specified according to application requirements, while the choice of block size is a tradeoff between image quality and imaging time. Smaller block size means less imaging time for each block, which implies less drift effect within each image. However, too small blocks will result in more block numbers and more scanning time. The robustness of the proposed method will be hurt too.

After the parameters are selected, the entire region to be imaged has to be split into blocks by resorting to following rules.

1. All blocks combined together should cover the whole region of the sample.

2. Each block should overlap with at least one other block with certain area.

A straightforward example of allocating blocks is illustrated in Fig. 3. Apparently, block 1 overlaps block 2 at its right side.

Without loss of generality, assume that the scanned region and small blocks are all squares. Let the sizes of the whole image and the block are L and l respectively. Then, the height data of the entire scanned region can be written as

$$h(x,y) \qquad 0 \le x \le L-1,\ 0 \le y \le L-1 \tag{1}$$

Moreover, the ith block can be also represented as

$$h_i(x,y) = h(x_i + x, y_i + y) \qquad 0 \le x \le l-1, 0 \le y \le l-1 \tag{2}$$

x_i and y_i denote the initial pixel's coordinate (the upper left corner) of the ith block. It means that the ith block covers pixels with x-axis of x_i to x_i *+l-1* and y-axis of y_i to y_i *+l-1*. Apparently, x_1 and y_1 are equal to 0 for block 1, and the values of x_i and y_i ($i \neq 1$) can be determined from Fig. 3.

Subsequently, all blocks are imaged by AFM according to the order denoted in Fig. 3.

3.2 Block Overlap Localization

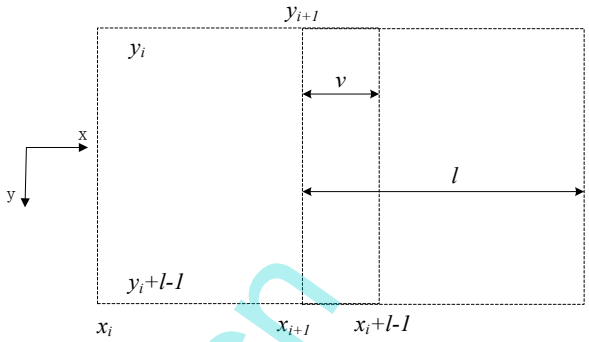

(a) Horizontal overlapping

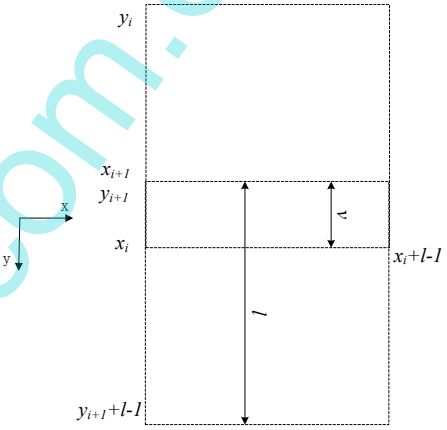

(b) Vertical overlapping

Fig. 4. Two overlapping scenarios for two successive blocks.

In this subsection, the overlapping areas between successive blocks have to be localized for further process. Without loss of generality, take the ith and *(i+1)*th image blocks for instance. There could be two overlapping scenarios, which can be seen in Fig. 4. Assume that the width of the overlapping fragment is designated to be v. First, they could overlap with each other horizontally as shown in Fig. 4(a). The area within block i overlapping with block j can be written as

$$h_{oij}(x,y) = h_i(x+l-v, y) = h(x_i + x + l - v, y_i + y) \qquad 0 \le x \le v-1, 0 \le y \le l-1 \tag{3}$$

Similarly, the area within block j overlapping with block i can be written as

$$h_{oji}(x,y) = h_j(x,y) = h(x_j + x, y_j + y) \qquad 0 \le x \le v-1, 0 \le y \le l-1 \tag{4}$$

In second scenario, the ith and *(i+1)*th image blocks overlap with each other vertically, as depicted in Fig. 4(b). In this case, the area within block i overlapping with block j can be written as

$$h_{oij}(x,y) = h_i(x, y+l-v) = h(x_i + x, y_i + y + l - v) \qquad 0 \le x \le l-1, 0 \le y \le v-1 \tag{5}$$

while the area within block *j* overlapping with block *i* is

$$h_{oji}(x,y) = h_j(x,y) = h(x_j + x, y_j + y) \quad 0 \le x \le l-1, 0 \le y \le v-1 \tag{6}$$

3.3 Drift Calculation

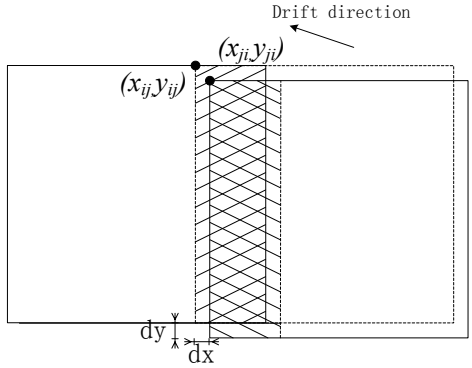

Fig. 5. Illustration of the difference between the desired and actual overlapping area

In previous subsection, two successive image blocks with overlapping area have been attained. Without loss of generality, take horizontal overlapping as example. Ideally, if there is no thermal drift present, the overlapping area should stay same for both of blocks, i.e.,

$$h_{oij}(x,y) = h_{oji}(x,y) \tag{7}$$

or equivalently,

$$\begin{aligned} &h(x_{ij} + x, y_{ij} + y) = h(x_{ji} + x, y_{ji} + y) \\ &x_{ij} = x_{ji}, \quad y_{ij} = y_{ji} \end{aligned} \tag{8}$$

where the initial pixel coordinates are defined as

$$\begin{cases} x_{ij} = x_i + l - v, & y_{ij} = y_i \\ x_{ji} = x_j, & y_{ji} = y_j \end{cases} \tag{9}$$

However, due to temperature change in ambient environment, the AFM tip drifts with time even if all scanning parameters remain unaltered. Therefore, there will be a translational movement between adjacent two blocks as illustrated in Fig. 5. The dashed square represents the place where block *j* is supposed to be when no drift is assumed. The right solid square represents the actual region where block *j* is located. It can be evidently found that due to drift effect, there exist a displacement between them, which is quantified as *dx* and *dy*. That is to say, the initial pixel coordinates satisfy

$$\begin{aligned} x_{ji} &= x_{ij} + dx \\ y_{ji} &= y_{ij} + dy \end{aligned} \tag{10}$$

Afterwards, the drift between block *i* and *j* will be estimated by phase correlation method, so that they can be combined with each other later.

A. Gradient Image

As it has been recognized that drift takes place in all three dimensions. Ideally, the height data between the overlapping fragments of the two adjacent blocks can be written as

$$h_{oji}(x,y) = h_{oij}(x + dx, y + dy) + dz \quad 0 \le x \le v-1,\ 0 \le y \le l-1 \tag{11}$$

where *dx, dy, dz* denote drift between the *i*th and the *j*th image blocks in the *x, y, z* axis respectively.

Before phase correlation method can be employed to estimate horizontal displacement, vertical drift has to be offset. To this end, a gradient image has to be calculated as for the overlapping fragments (Yang et al, 2008)

$$g_{ij}(x,y) = \begin{cases} h_{ij}(x,y) & \text{if} \quad x = 0,\ 0 \le y \le L-1 \\ h_{ij}(x,y) - h_{ij}(x-1,y) & \text{others} \end{cases} \tag{12}$$

$$g_{ji}(x,y) = \begin{cases} h_{ji}(x,y) & \text{if} \quad x = 0,\ 0 \le y \le L-1 \\ h_{ji}(x,y) - h_{ji}(x-1,y) & \text{others} \end{cases} \tag{13}$$

By this means, the negative drift effect on *z* axis can be largely reduced.

B. Phase Correlation Method

Phase correlation method measures the motion directly from the phase correlation map. It can figure out an accurate and robust estimation of the motion vector with much lower entropy (Stiller, et al, 1999). It is widely used in the field of signal processing and computer image processing to estimate and compensate motion displacement thanks to its robust performance and relax of requirement on object identification.

In the proposed scheme, to achieve more accurate result, a normalization and grey-scale transformation step is conducted to all image fragments.

$$g_{ij}'(x,y) = \frac{g_{ij}(x,y) - \min(g_{ij}(x,y))}{\max(g_{ij}(x,y)) - \min(g_{ij}(x,y))} \tag{14}$$

$$g_{ij}''(x,y) = \begin{cases} 0.6 * (1 - \exp(g_{ij}'(x,y))) + 0.5 & \text{if } g_{ij}'(x,y) > 0.5 \\ 0.6 * (1 - \exp(g_{ij}'(x,y))) + 0.5 & \text{if } g_{ij}'(x,y) \le 0.5 \end{cases} \tag{15}$$

The pre-process transformation can highly enhance the accuracy and robustness of the outcome of the phase correlation method, of which the basic principle is briefly discussed next.

Assume that there exists a translational shift between image fragment *i* and *j*, which can be rewritten as

$$g_{ji}''(x,y) = g_{ij}''(x + dx, y + dy) \tag{16}$$

Taking 2-D Fourier transform of (16) yields

$$G_{ji}(f_x, f_y) = G_{ij}(f_x, f_y) \cdot \exp[j2\pi(dx \cdot f_x + dy \cdot f_y)] \tag{17}$$

Therefore, the displacement in the spatial domain is transformed into the frequency spectrum domain along with a phase change. Thence, the cross correlation between any two image fragments can be written as

$$c_{i,j}(x,y) = g_{ji}''(x,y) \cdot g_{ij}'''^{*}(-x,-y) \tag{18}$$

The Fourier transform of (18) is

$$C_{i,j}(f_x, f_y) = G_{ji}(f_x, f_y) \cdot G_{ij}^{*}(f_x, f_y) \tag{19}$$

After normalizing the cross-power spectrum by its magnitude, we obtain its phase as

$$\Phi[C_{i,j}(f_x, f_y)] = \frac{G_j(f_x, f_y) G_i^{*}(f_x, f_y)}{\left| G_j(f_x, f_y) G_i^{*}(f_x, f_y) \right|} \tag{20}$$

By substituting (17) into (20), we obtain

$$\Phi[C_{i,j}(f_x, f_y)] = \exp[-j2\pi(dx \cdot f_x + dy \cdot f_y)] \tag{21}$$

The 2-D inverse Fourier transform of (21) is

$$c_{i,j}(x, y) = \delta(x - dx, y - dy) \tag{22}$$

where $\delta(\cdot)$ is an impulse function which can be readily localized on the *x*-*y* plane. Thus, the motion vector can be computed according to the position of the impulse function. Finally, the stitching method can be carried out to combine all blocks, which will be stated later.

Fig. 6 depicts how to calculate the drift of two successive image blocks. There are two image blocks (a) and (b). The designed overlap is circled by a black-edge rectangular. (c) shows the Obtain the overlap image fragment. Then, the phase correlation method is adopted to calculate the drift of the gradient images, which is illustrated in (d). Once the drift of two overlap image fragments is calculated out, it's easy to stitching them together.

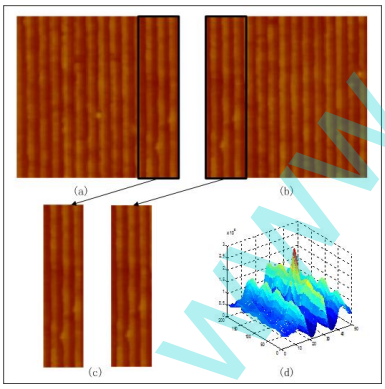

Fig. 6. The process of calculating the drift of two successive image blocks.

3.4 Stitching method

Once the estimated drift between successive image blocks is computed, we can easily stitch two images together. To complete the splicing process, we first define a blank and big enough image canvas, and then paste the scanned image blocks onto it in sequence. All procedure can be detailed as follows.

Firstly, define a image canvas which has enough pixels to cover the original scanned region, and it is defined as *canvas(x,y)* .

Secondly, paste the first image block on upper left corner of the canvas. Leave a certain margin to the canvas boundary. Define the margin dimension as x_1, y_1. Thus, it follows that

$$Canvas(x + x_1, y + y_1) = h_1(x, y) \quad 0 \le x \le l-1,\ 0 \le y \le l-1 \tag{23}$$

where $h_1(x,y)$ is the first scanned image block.

Subsequently, the other blocks will be attached to the canvas in sequence of the order by which they are imaged. If block *j* overlaps with block *i* horizontally, by recalling (3)(4)(9)(10), one has

$$h_{oij}(x, y) = h_{oji}(x + dx, y + dy) \tag{24}$$

Since *dx, dy* have been successfully estimated in previous step, block *j* can be attached to block *i* on the right by adjust its initial pixel coordinates by *dx, dy*. Similar routines can be also performed for blocks overlapping vertically.

Finally, once all image blocks are pasted onto the canvas, an integral topography image with high resolution is obtained for the original scanned region of the sample.

4. IMPLEMENTATION AND EXPERIMENT RESULTS

The following results have been obtained on a commercial AFM (BenYuan Co. Ltd.) operating in tapping mode. A grating sample with model 3600l is used for imaging purpose. The experiment is operated in ambient conditions, i.e., at room temperature and humidity.

In our experiment, a 9um*9um area is scanned with a resolution of 4086*4086, i.e., $L = 4086$. The size of the block is set as 2048*2048 representing an area of 4um*4um and $l = 2048$. Therefore, 9 image blocks are needed to cover the whole region. Overlap of two consecutive image blocks is set as a quarter of the block size, which means $v = 512$. To alleviate the effect of creep, the sequence to scan these images can be z-shaped, which means the sequence in the first and third lines is from left to right, but right to left in the second line.

The whole process of stitching all 9 images in sequence is depicted in Fig. 7. And finally, an image of the whole region with high resolution is obtained in Fig. 8. Apparently, compared with Fig. 1, a lot less distortion is present, which also verifies the feasibility of our proposed method.

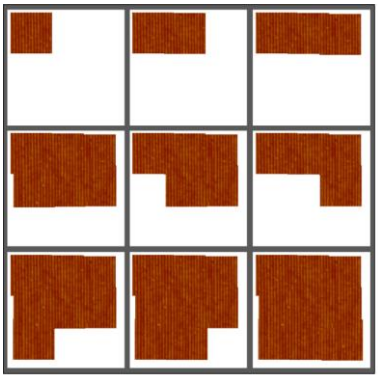

Fig. 7. The whole process of stitching all 9 images. The sequence to scan these images is z-shaped.

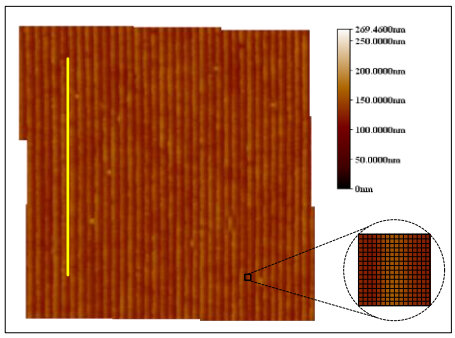

Fig. 8. The final large scale image with high resolution. Less distortion is observed compared with Fig. 1.

5. CONCLUSION

This paper presents an automatic block scan and stitching method to overcome nonlinearities during imaging process of AFM, especially when topography of a large scale of area is required along with high definition. By dividing the whole area into small blocks, creep and drift existing within an image can be largely reduced. Afterwards, the thermal drift between successive blocks is estimated using phase correlation method, and the whole image can be finally achieved by combining (stitching) all blocks together. This methodology can be utilized for various applications in different fields. Future work includes refining the block scale selection and drift calculation.

ACKNOWLEDGEMENT

This work is supported by National Natural Science Foundation (NNSF) of China under Grant 61104008, National High Technology Research and Development Program of China (863) under Grant 2012AA062201, and Research Fund for the Doctoral Program of Higher Education of China under Grant 20110101120063.

REFERENCES

Binnig, G. and Rohrer, H. (1983). "Scanning tunneling microscopy". *Surface Science*, vol. 126, pp. 236-244.

Fleming, A.J. and Moheimani, S.O.R. (2006) . "Sensorless vibration suppression and scan compensation for piezoelectric tube nanopositioners". *IEEE. Trans. Contr. Syst. Technol*., vol. 14, no. 1, pp. 33–44.

Goldfarb, M. and Celanovic, N. (1997). "Modeling piezoelectric stack actuators for control of micromanipulation". *IEEE Contr. Syst. Mag.*, vol. 17, no. 3, pp. 69–79.

Huerth, S.H. and Hallen, H.D. (2003). "Quantitative method of image analysis when drift is present in a scanning probe microscope". *J. Vac. Sci Technol. B*, vol. 21, no. 2, pp. 714–718.

Marinello, F., Bariani, P., Chiffre, L.De. and Savio, E. (2007). "Fast technique for AFM vertical drift compensation". *Meas. Sci. Technol*, vol. 18, pp. 689-696.

Mokaberi, B. and Requicha, A.A.G. (2006). "Drift compensation for automatic nanomanipulation with scanning probe microscopes". *IEEE Trans. on Automation Science & Engineering*, Vol. 3, No. 3, pp. 199-207.

Mokaberi, B. and Requicha, A.A.G. (2008). "Compensation of Scanner Creep and Hysteresis for AFM Nanomanipulation". *IEEE Trans. on Automation Science & Engineering*, vol. 5, no. 2, pp. 197-206.

Requicha, A.A.G. (2003). "Nanorobots, NEMS and nanoassembly". *Proc. IEEE*, vol. 91, no. 11, pp. 1922–1933.

Stiller, C. and Konrad, J. (1999). "Estimating Motion in Image Sequences". *IEEE Signal Processing Magazine*, vol. 16, no. 4, pp.70-91.

Yang, Q. and Jagannathan, S. (2006). "Atomic force microscope-based nanomanipulation with drift compensation". *Journal of Nanotechnology*, vol. 3, no. 4, pp. 5